

# Where am I? Cross-View Geo-localization with Natural Language Descriptions

Junyan Ye<sup>1,2\*</sup>, Honglin Lin<sup>2\*</sup>, Leyan Ou<sup>1</sup>, Dairong Chen<sup>4,1</sup>, Zihao Wang<sup>1</sup>, Conghui He<sup>2,3</sup>, Weijia Li<sup>1†</sup>  
<sup>1</sup>Sun Yat-Sen University, <sup>2</sup>Shanghai AI Laboratory, <sup>3</sup>Sensetime Research, <sup>4</sup>Wuhan University

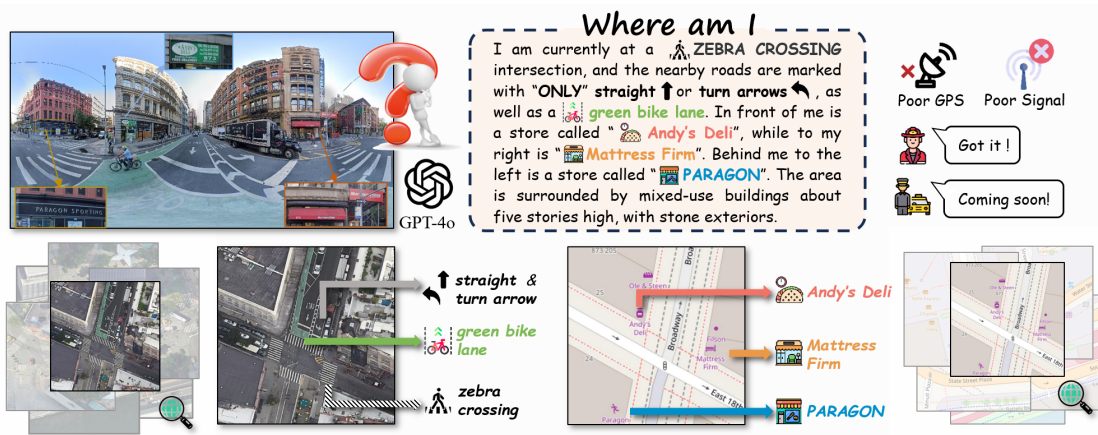


Figure 1. **Towards Text-guided Geo-localization.** In scenarios where GPS signals are interfered with, users must describe their surroundings using natural language, providing various location cues to determine their position (*Up*). To address this, we introduce a text-based cross-view geo-localization task, which retrieves satellite imagery or OSM data based on textual queries for position localization (*Down*).

## Abstract

*Cross-view geo-localization identifies the locations of street-view images by matching them with geo-tagged satellite images or OSM. However, most studies focus on image-to-image retrieval, with fewer addressing text-guided retrieval, a task vital for applications like pedestrian navigation and emergency response. In this work, we introduce a novel task for cross-view geo-localization with natural language descriptions, which aims to retrieve corresponding satellite images or OSM database based on scene text. To support this task, we construct the CVG-Text dataset by collecting cross-view data from multiple cities and employing a scene text generation approach that leverages the annotation capabilities of Large Multimodal Models to produce high-quality scene text descriptions with localization details. Additionally, we propose a novel text-based retrieval localization method, CrossText2Loc, which improves recall by 10% and demonstrates excellent long-text retrieval capabilities. In terms of explainability, it not only provides similarity scores but also offers retrieval reasons. More information can be found at <https://yejy53.github.io/CVG-Text/>.*

<sup>†</sup>Corresponding author. \* Equal contribution.

## 1. Introduction

Accurate positioning of ground-level images is crucial for various applications, including pedestrian navigation [36], mobile robot localization [32], and noisy GPS signals correction in crowded urban areas [37]. Traditional localization methods typically rely on 3D point cloud positioning [16, 25] or cross-view retrieval using GPS-tagged satellite images [10, 44, 45]. However, most research focuses on matching image-to-3D data or image-to-image data. Recent studies have begun to explore a novel localization approach based on natural language text, which holds significant value for many practical applications [36, 39, 40, 43]. As shown in Figure 1, taxi drivers rely on verbal instructions from passengers to determine their location [19], or pedestrians describe their position during emergency calls [7].

Recent natural language localization methods, such as Text2Pose[19] and Text2Loc [40], have been limited to using natural language to identify individual locations within point clouds. Constructing 3D maps using LiDAR or photogrammetry is expensive on a global scale [1, 13, 27], and the storage costs for 3D maps are also high, often requiring costly cloud infrastructure, which hinders localization on mobile devices. Notably, the cross-view retrieval geo-

localization paradigm [41, 45, 53] that utilizes OSM<sup>1</sup> map data or satellite imagery, although oriented towards coarse-grained localization, can still meet the needs of most tasks and has clear advantages over 3D data in terms of coverage and storage costs. Therefore, this paper introduces a novel cross-view geo-localization task, i.e., exploring the use of natural language descriptions to retrieve corresponding OSM or satellite images.

To tackle this challenging task, a dataset is needed that (i) contains foundational cross-view data with street-view, OSM, and satellite images, and (ii) includes text data capable of simulating human users in describing street-view scenes, while providing high-quality scene localization cues. With the development of large multimodal models (LMMs), annotating text using LMMs seems to be an effective solution [4, 8, 14]. However, LMMs may suffer from vague descriptions or hallucination phenomena [15, 31]. To address these issues, we propose the Cross-View Geo-localization dataset, CVG-Text. We first collected street-view data from over 30,000 locations in three cities, New York, Brisbane, and Tokyo. Then, based on the geographical coordinates, we obtained corresponding paired data of OSM and satellite images. Subsequently, we developed a progressive text description framework that leverages LMM, GPT-4o [28] as the core for generation, combining Optical Character Recognition (OCR) [26] and Open-World Segmentation [29, 49] techniques to generate high-quality scene description text from street-view images while reducing vague descriptions.

Although the textual data constructed above can provide user-like street scene descriptions, it still has still have a significant domain gap compared to satellite images or OSM data. Moreover, in order to fully capture the scene’s detailed information, the generated text descriptions are generally long, often exceeding the text encoding limits of image-text retrieval methods. To address this issue, we propose a novel Cross-view Text-based Localization method, *Cross-Text2Loc*. This method includes a length-extended text encoding module, Extended Embedding, which fully leverages the long and complex text descriptions in the dataset. Through contrastive learning strategies, it effectively learns cross-domain matching information. It also features an Explainable Retrieval Module (ERM), which provides natural language explanations alongside the retrieval results. This overcomes the limitations of traditional cross-view retrieval methods that only provide similarity scores, lacking interpretability and making it difficult to make confident decisions. We evaluate the performance of mainstream text-image retrieval methods and our method on this novel task, and the experimental results demonstrate that our *Cross-Text2Loc* has significant advantages in recall metrics and interpretability. Our main contributions are as follows:

- We introduce and formalize the Cross-View Geo-localization task based on natural language descriptions, utilizing scene text descriptions to retrieve corresponding OSM or satellite images for geographical localization.
- We propose *CVG-Text*, a dataset with well-aligned street-views, satellite images, OSM, and text descriptions across three cities and over 30,000 coordinates. Additionally a progressive scene text generation framework based on LMM is presented, which reduces vague descriptions and generates high-quality scene text.
- We introduce *CrossText2Loc*, a novel text localization method that excels in handling long texts and interpretability. It achieves over a 10% improvement in Top-1 recall compared to existing methods, while offering retrieval reasoning beyond similarity scores.

## 2. Related Work

### 2.1. Cross-view Geo-localization

Cross-view geo-localization identifies the geographic locations of street-view images by matching them with geographic reference satellite databases or OSM databases for coarse localization [22, 23, 34, 41, 45]. For example, works like Sample4G [10] employ a contrastive learning framework to match features of street-view images with satellite image features, achieving high-accuracy satellite data retrieval. However, current cross-view retrieval and localization tasks primarily focus on image-to-image, with limited consideration for text, which presents certain shortcomings in practical applications. Additionally, existing cross-view retrieval methods mainly provide similarity score, with little research dedicated to confident and interpretable retrieval localization. Our proposed text retrieval localization task is based on the retrieval and localization of natural language, addressing the gap in existing research regarding text-guided scene localization applications. This approach enables more transparent and interpretable retrieval localization through the use of natural language.

### 2.2. Visual Language Navigation and Localization

Visual Language Navigation (VLN) requires agents to navigate specific environments based on natural language instructions [2, 6]. Previous tasks have primarily focused on decision-making based on images and natural language. Recent works have begun to shift from visual language navigation to direct visual language localization tasks. For instance, Loc4Plan [36] emphasizes the necessity of visual spatial localization prior to navigation. Text2Pose [19] and Text2Loc [40] explore the use of natural language to identify individual positions in outdoor point cloud maps. However, point cloud retrieval tasks tend to incur high storage and computational costs when handling large-scale areas. In contrast, our task retrieves corresponding satellite images

<sup>1</sup><https://www.openstreetmap.org/>

or OSM data based on text queries, allowing for broad area coverage while reducing storage and computational costs.

### 2.3. Data Synthesis via LMMs

The rapid development of multimodal large models (LMMs) has demonstrated their outstanding ability to generate high-quality natural language descriptions [3, 28, 35, 52]. Many studies have leveraged LMMs for automated data annotation [14], such as LatteCLIP [4], which synthesizes text using LMMs for unsupervised CLIP fine-tuning. However, text retrieval localization tasks impose higher demands on the annotation capabilities of LMMs, requiring them to accurately identify key localization details in street-view images, such as store signs and other critical information, while minimizing interference from hallucination phenomena [15, 31, 46].

In our fine-grained text synthesis, we incorporate street-view image input, OCR [26], and open-world segmentation [29] to enhance GPT’s information capture capability and reduce hallucination. Additionally, we carefully designed system prompts to guide GPT in generating fine-grained textual descriptions based on a progressive scene analysis chain of thought.

ined textual descriptions.

### 2.4. Multi-modality Alignment

In this work, our task involves retrieving satellite images or OSM images based on scene text descriptions synthesized by LMMs, which can be seen as a subtask of text-to-image retrieval [9, 11, 21, 42, 51]. The CLIP [30] model introduced a contrastive learning approach between image-text pairs, establishing a new paradigm for recent text retrieval tasks. However, such models often have fixed maximum sequence length limitations, typically defaulting to 77 tokens, making it challenging to handle complex long-text scene descriptions. This can lead to the loss of fine-grained textual information, negatively impacting model performance. Inspired by works like Long-CLIP [48], our retrieval method employs stretching to extend the model’s acceptable text length, enabling the retrieval of long text descriptions for environmental contexts.

## 3. CVG-Text Dataset

### 3.1. Overview

We introduce CVG-Text, a multimodal cross-view retrieval localization dataset designed to evaluate text-based scene localization tasks. CVG-Text covers three cities: New York, Brisbane, and Tokyo, encompassing over 30,000 scene data points. The data from New York and Tokyo is more oriented toward urban environments, while the Brisbane data leans towards suburban scenes. Each individual point includes

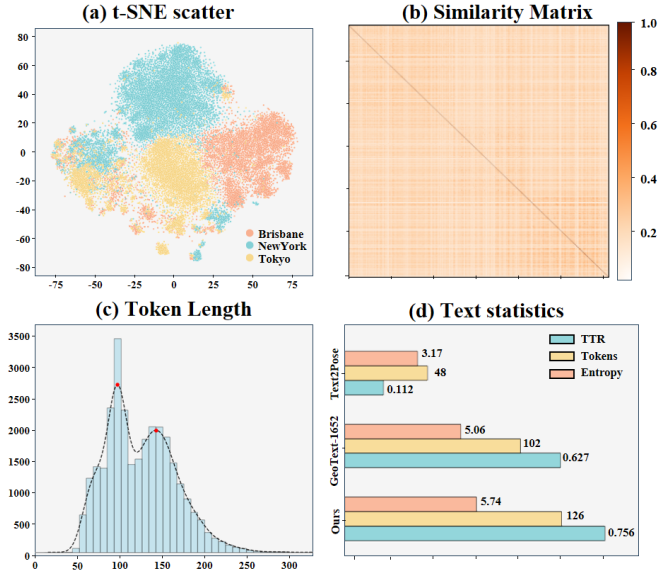


Figure 2. **Textual Feature Statistics Overview.** (a) t-SNE visualization of text data from different cities; (b) text similarity matrix; (c) token length distribution histogram; (d) comparison of text statistics across different datasets.

corresponding street-view images, OSM data, satellite images, and associated scene text descriptions. The dataset is randomly split into training and test sets with a ratio of 5:1. More details can be found in the supplementary materials.

**Statistical Overview of Text Data.** Figure 2 presents the feature statistics of the scene text. The t-SNE dimensionality reduction visualization indicates a relatively dispersed distribution of the text data, reflecting high diversity. Texts from the same city exhibit clustering, while texts from different cities are clearly distinguishable, highlighting regional variations in text features. These differences are likely tied to the unique styles and cultural characteristics of each city. The text similarity matrix reveals low similarity, demonstrating the independence of the texts, which effectively represent each distinct scene and reduce the risk of confusion between different texts. The average text length generated by the multimodal large model GPT-4o exceeds 126 tokens, with two prominent peaks at 100 and 145 tokens, corresponding to single-view and panoramic images, respectively. Compared to datasets such as Text2Pose and GeoText-1652, our data shows superior performance in vocabulary richness, token length, and entropy, reflecting a higher quality of text.

**Comparisons with Existing Datasets.** Table 1 provides a detailed comparison between CVG-Text and existing datasets. In contrast to common cross-view retrieval datasets, such as CVUSA [38] and VIGOR [53], CVG-Text includes aligned text modality information, enabling the evaluation of text-based scene localization tasks and interpretability analysis for cross-view retrieval. Further-

Table 1. Comparison of the proposed CVG-Text with existing cross-view datasets. # Ref. and # G-Query represent the number of reference images and ground query images, respectively.

Dataset	Text	Pano <sup>1</sup>	Single <sup>2</sup>	OSM	# Ref.	# G-Query
CVUSA [38]		✓			44k	44k
CVACT [24]		✓			128k	128k
Uni.-1652 [50]			✓		90k	14K
VIGOR [53]		✓			105k	90k
CVGlobal [45]		✓		✓	130K	130K
Geotext-1652 [9]	✓		✓		90k	14K
Ours	✓	✓	✓	✓	60k	30k

<sup>1</sup> Pano refers to the Panoramic street-view images.

<sup>2</sup> Single refers to the Single-view street-view images.

more, CVG-Text demonstrates superior data completeness, encompassing panoramic street-views, single-perspective street-views, aerial images, and OSM data.

Compared to GeoText-1652 [9] dataset, which is primarily used for drone navigation, the text descriptions are directly derived from drone images and are used for drone image retrieval. Our task, however, focuses on addressing the needs of pedestrians, tourists, and other users, with text originating from street-view images and used for cross-domain retrieval of satellite or OSM images. There is a significant difference in both task objectives and the source of text. Furthermore, the coverage of drone images is more limited compared to the OSM and satellite images, making it difficult to achieve large-scale geo-localization.

### 3.2. Data Collection

We collected panoramic and single-perspective street-view images from different city areas using the Google Street View <sup>2</sup> and Google Places API <sup>3</sup>. The resolution of the panoramic street-view images is  $2048 \times 1024$ , with the north direction aligned to the middle column. The resolution of the single-perspective images is not fixed, but all are high-definition images. Based on the latitude and longitude coordinates of the street-view images, we collected corresponding satellite image tiles using Google Maps API<sup>4</sup>. The size of the satellite images is  $512 \times 512$ , with a zoom level of 20 and a ground resolution of around 0.12m, aligned with the center of the street-view images.

Additionally, we collected corresponding OSM data for each region in vector format, encompassing global geographic and map information. OSM data contains numerous points of interest (POIs) with rich label information, such as restaurant names and bus stops, which are highly useful for geo-localization tasks. We utilize raster tiles provided by the OSM official website as retrieval targets, retaining various POI identifiers. The size of the OSM raster data

<sup>2</sup><https://www.google.com/streetview/>

<sup>3</sup><https://developers.google.com/maps/documentation/places/web-service>

<sup>4</sup><https://www.google.com/maps>

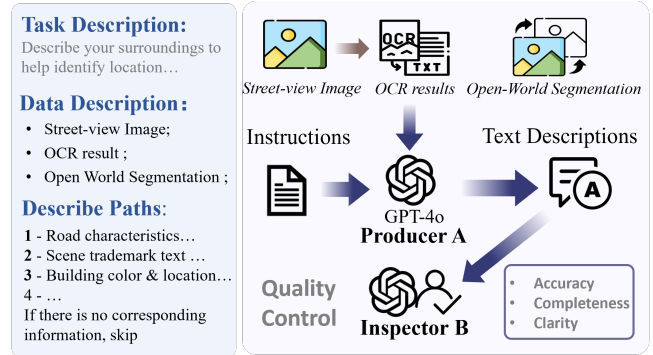


Figure 3. Overall Process for Street-View Text Description Generation using GPT-4o.

is  $512 \times 512$ , which is close to the image size and corresponding geographical extent of the satellite images. Since OSM data is dynamically updated, we collected street-view data from recent years to minimize discrepancies between the OSM and street-view data. Existing cross-view datasets typically include street-view data from before 2021; thus, rather than adding text annotations to existing datasets, we opted to collect new data.

### 3.3. Text Data Synthesis

Figure 3 illustrates the main process of text synthesis based on GPT-4o. We first utilize Paddle OCR<sup>5</sup> to capture text within street-view images, enabling GPT to focus on key semantic text information present in the images while reducing hallucination phenomena. Additionally, we perform open-world segmentation on the street-view images to provide more semantic details and location information for the subsequent text synthesis process. With the help of the semantic segmentation results, OCR outputs related to moving objects, such as vehicles, can also be filtered out. Next, we designed a systematic prompting scheme to generate scene text descriptions using GPT-4o. The system prompts are divided into four parts: task requirements, input data introduction, description paths, and response demands. Specifically, we employ a progressive scene analysis strategy to guide GPT in sequentially describing road features, building signage, and the overall environment, including aspects such as color, material, and distribution. In real-world applications, users may not know the exact geographic orientation. Therefore, text descriptions often use simple directional cues like front, back, left, and right to describe the scene. More implementation details can be found in the supplementary materials.

In terms of quality control, we first filter out incorrectly formatted responses and conduct GPT-based review of both images and textual descriptions to ensure accuracy, consistency, content completeness, relevance, clarity, and com-

<sup>5</sup><https://github.com/PaddlePaddle/PaddleOCR>

prehensiveness. Samples that do not meet the standards are re-synthesized. Additionally, we extracted 20% of the samples (approximately 6,000) for manual expert review, involving 10 human evaluators and requiring around 100 hours of work. The pass rate for the manual checks was 77.6%. Furthermore, street-view retrieval experiments using a retrained CLIP model showed that the Top-1 recall rate for text-to-street view was over 85.5%, validating the high quality of the dataset’s text descriptions.

## 4. Method

### 4.1. Overview

**Problem Formulation.** In this work, we introduce a novel task for cross-view geo-localization with natural language. The objective of this task is to leverage natural language descriptions to retrieve its corresponding OSM or satellite images, of which the location information is usually available. The input for this task is a text description  $Q\text{-Text}$  describing a street scene. As the text describes the scene corresponding to a street-view image, a key challenge is the significant domain discrepancy between street-view images and satellite or OSM data. In practical applications, users often have location prior, such as knowing they are in a particular district of New York City, but not the precise location. Therefore, the retrieval model utilizes this location prior to narrow the search scope  $M$ , querying a smaller subset of satellite images,  $R\text{-sat}$ , and OSM image,  $R\text{-OSM}$ .

**Model Architecture.** To address the challenge of the task, we propose the CrossText2Loc architecture (Figure 4). Our model adopts a dual-stream architecture, consisting of a visual encoder and a text encoder. Specifically, the architecture incorporates an Expanded Positional Embedding Module (EPE) and a contrastive learning loss  $L_{itc}$  to facilitate long-text contrastive learning. Additionally, we introduce a novel Explainable Retrieval Module (ERM), which includes attention heatmap generation and LMM interpretation, to provide natural language explanations, enhancing the interpretability of the retrieval process.

### 4.2. Long-text Contrastive Learning

**Expanded Positional Embedding.** To address the challenge of complex long scene text in cross-modal retrieval tasks, we employ a Extended Positional Embedding Module (EPE) for long-text encoding. Due to the scene texts in our case are generated by GPT for simulating user data, there are no prominent short titles at the beginning which carry significant importance. Therefore, unlike LongCLIP [48] uses Knowledge Preserving Stretching, we use a full interpolation method.

Specially, we utilize linear interpolation to expand the positional embeddings within the text encoder to accommodate a sequence length of  $N$  (300) tokens. The expanded

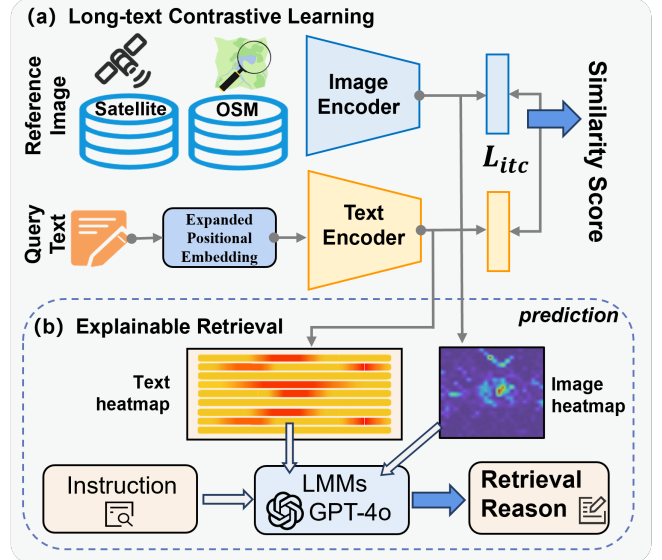


Figure 4. **The proposed CrossText2Loc method.** Street-view texts serve as query inputs, with satellite and OSM images as references. The blue arrows point to the output results, including similarity score and retrieval reason.

positional embedding  $P^*$  can be computed from the original positional embedding  $P$  as follows:

$$P^*(x) = (1 - (x - \lfloor x \rfloor)) \cdot P(\lfloor x \rfloor) + (x - \lfloor x \rfloor) \cdot P(\lceil x \rceil) \quad (1)$$

Where  $P^*(x)$  represents the expanded positional embedding at position  $x$ ,  $P(\lfloor x \rfloor)$  and  $P(\lceil x \rceil)$  are the values from the original positional embedding at the indices  $\lfloor x \rfloor$  and  $\lceil x \rceil$ , with  $\lfloor \cdot \rfloor$  and  $\lceil \cdot \rceil$  denoting the floor and ceiling functions respectively.

By extending the positional embeddings of the text encoder, our model is capable of processing longer text inputs, allowing it to capture a complete context.

**Image-text Contrastive Learning.** We align the embedding spaces of images and long text descriptions through contrastive learning, as shown in Figure 4 (a). Specifically, we set the batch size to  $n$  and align the representations of images and text by minimizing the contrastive learning loss function  $L_{itc}$ . To achieve this, we uniformly encode panoramic and single-view texts as  $t$ , and satellite and OSM images as  $v$ . The loss function is expressed as:

$$L_{itc} = \sum_{i=1}^n \sum_{j=1}^n -\log \frac{\exp(\text{sim}(v_i, t_j)/\tau)}{\sum_{k=1}^n \exp(\text{sim}(v_i, t_k)/\tau)} \quad (2)$$

Where  $v_i$  and  $t_j$  represent the  $i$ -th image and the  $j$ -th text embedding vector respectively.  $\tau$  is a learnable temperature used to control the sharpness of softmax distribution.

### 4.3. Explainable Retrieval Module (ERM)

We propose the Explainable Retrieval Module (ERM) to enhance the interpretability of geo-localization with natural

Method	Satellite image						OSM data					
	NewYork		Brisbane		Tokyo		NewYork		Brisbane		Tokyo	
	R@1	L@50	R@1	L@50	R@1	L@50	R@1	L@50	R@1	L@50	R@1	L@50
ViLT[17]	11.58	15.58	11.00	14.50	10.83	15.50	5.83	9.92	8.67	11.75	4.67	9.17
SigLIP-B/16[47]	19.67	21.08	19.58	22.00	15.58	17.92	20.17	21.58	25.58	27.42	11.92	13.67
SigLIP-SO400M[47]	33.50	34.83	34.25	36.83	28.42	31.50	27.75	29.58	29.75	31.58	17.50	19.50
EVA2-CLIP-B/16[12]	25.17	26.58	28.42	31.75	22.50	25.25	18.58	20.83	27.33	28.83	13.92	15.67
EVA2-CLIP-L/14[12]	34.08	35.67	35.67	38.00	31.00	34.08	26.33	28.67	30.92	32.67	19.83	22.50
BLIP[20]	34.58	37.25	34.50	38.17	29.75	33.67	52.92	55.92	43.00	46.33	30.67	34.50
CLIP-B/16[30]	26.67	28.17	29.92	32.58	24.00	27.25	27.42	29.42	30.83	32.67	17.75	19.92
CLIP-L/14[30]	35.08	37.08	34.08	37.25	28.08	30.50	31.50	33.58	32.50	34.67	21.00	23.17
Ours	<b>46.25</b>	<b>48.75</b>	<b>43.58</b>	<b>47.42</b>	<b>36.83</b>	<b>39.58</b>	<b>59.08</b>	<b>62.00</b>	<b>46.08</b>	<b>48.67</b>	<b>34.33</b>	<b>38.33</b>

Table 2. **Quantitative comparison of different methods on CVG-Text.** R@1 represents the Top-1 image recall rate; L@50 represents the recall rate where localization error is less than 50 meters.

language during the inference time, as shown in Figure 4 (b). The module consists of two main components: Attention Heatmap Generation and LMM Interpretation.

**Attention Heatmap Generation.** Inspired by the method described in [5], we generate attention heatmaps to reveal the model’s focus during retrieval. Specifically, we initialize the correlation heatmap before the starting layer  $s$  with an identity matrix  $I$ . Then, we iteratively process each attention layer from the starting layer  $s$  to the output layer  $L$ . In each attention mechanism, we accumulate non-negative gradient contributions to generate attention heatmaps that highlight the regions the model focuses on. The image or text correlation heatmap  $R$  can be calculated as:

$$R^{(l)} = R^{(l-1)} + \frac{1}{H} \sum_{h=1}^H \max(0, \nabla A_h^{(l)} \odot A_h^{(l)}) R^{(l-1)} \quad (3)$$

Where  $A_h^{(l)}$  represents the attention weight of the  $h$ -th attention head at layer  $l$ ,  $\nabla A_h^{(l)}$  is the gradient of the attention weight,  $\odot$  denotes the Hadamard product,  $H$  is the total number of attention heads.

**LMM Interpretation.** After generating the image and text heatmaps, we feed them into the LMM (GPT-4o) with a carefully designed prompt. First, the LMM observes the heatmaps to identify key clues in the image and text that the model focuses on during retrieval, such as specific landmarks or geographical features. Then, the LMM compares and reasons over the highlighted regions in the text and image, providing an explanation for why the model retrieved the query in a particular way, i.e., the rationale behind the matching of the query and reference data. LMMs are capable of providing retrieval explanations in natural language, beyond just similarity measures, which is highly beneficial for the interpretability and trustworthiness of geo-localization retrieval. Even in cases where retrieval fails, the

model’s abnormal attention can help to further improve retrieval algorithm performance.

## 5. Experiment

### 5.1. Experimental setup

**Implementation Details.** We used the CLIP-L/14@336px model [30] pre-trained by OpenAI as the backbone, with the Adam optimizer [18], a learning rate of 1e-5, and cosine learning rate decay. The batch size was set to 128, and training was conducted over 40 epochs on four NVIDIA A100 GPUs. The image resolution was set to default  $336 \times 336$ , and the text context length  $N$  was 300 tokens. We initialized the temperature coefficient  $\tau$  from the checkpoint. The image resolution for all baseline methods followed their respective default optimal settings. Moreover, as mentioned in Section 4.1, based on practical application requirements and utilizing user location priors, we set the retrieval range  $M$  to 100. During testing, the reference database consists of 100 samples from the nearby area, covering an area of approximately 10 km<sup>2</sup>.  $M$  is a configurable parameter, and we present additional results with different  $M$  settings in the supplementary material.

**Evaluation Metrics.** Following previous cross-view geo-localization works [10, 33], we use the image recall accuracy of the top  $K$  images as an evaluation metric to assess text retrieval localization performance. Specifically, given a query text for a certain location, if its ground-truth OSM and satellite image is within the top  $K$  retrieval results, the location is considered “successfully localized.” Additionally, we also provide the localization recall rate metric [19, 40]. Similarly, the localization recall rate refers to the proportion of retrieved results where the distance to the actual location is below a specified threshold.

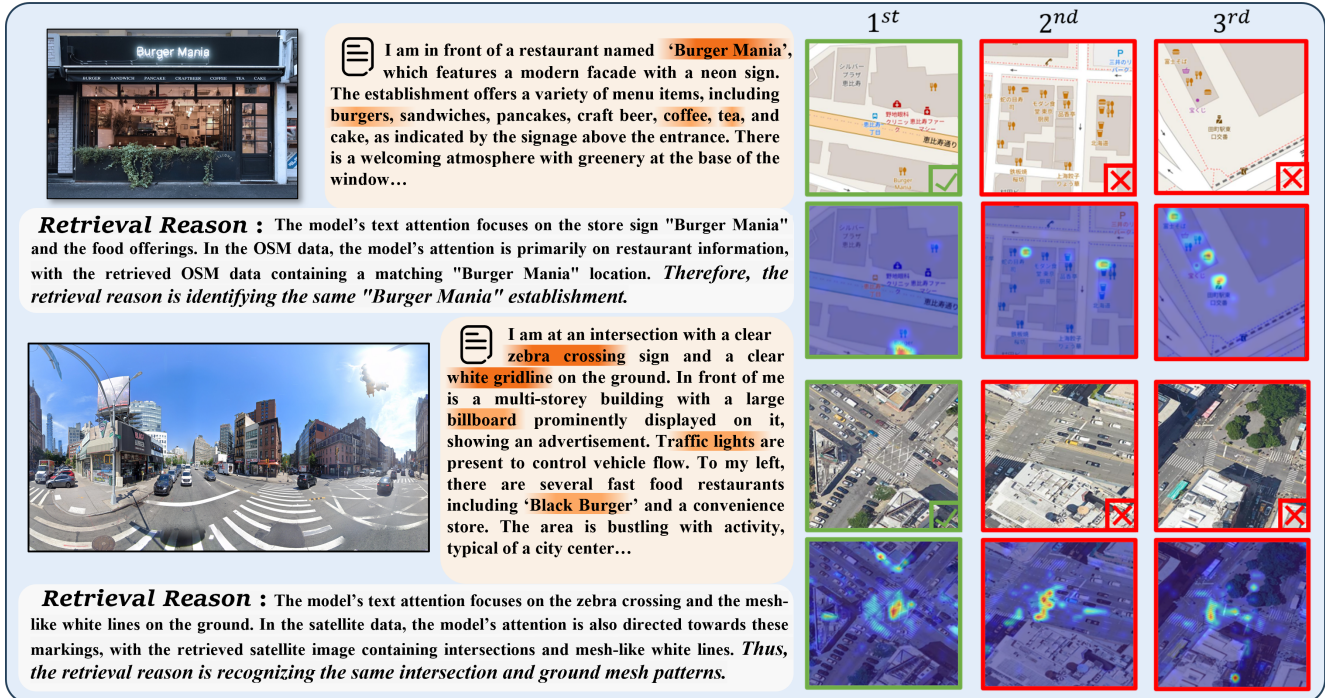


Figure 5. **Qualitative retrieval results on CVG-Text Dataset.** The left side of the figure displays the original street-view data, synthetic text data with corresponding response heatmaps, and retrieval reason provided by our ERM module. The right side shows the top three retrieval results with corresponding response heatmaps; green indicates correct matches and red denotes incorrect results.

## 5.2. Geo-localization Performance

We evaluated the performance of various text-based retrieval methods under different settings of satellite images and OSM data, with the results shown in Table 2. The methods with the same architecture tend to perform better as the number of parameters increases. Among the existing approaches, BILP achieves optimal performance, as it is not constrained by limitations on text embedding length. Our method achieved the best results, outperforming the baseline CLIP method by a 14.1% improvement in Image Recall R@1 and a 14.8% improvement in Localization Recall L@50, demonstrating its superiority for this task.

Next, we analyze the performance of our method in different cities. In the evaluation results for New York, we found that OSM significantly outperforms satellite imagery. This is because OSM data contains more POI information relevant to street view locations, such as bus stops, store names, etc., which are difficult to identify in satellite images. In contrast, the level of detail in OSM data for Brisbane is limited, and in this case, the localization performance of satellite images is comparable to that of OSM. In Tokyo, due to the poor pre-training of CLIP on Japanese, the model's response to certain Japanese words in the street view description text and Japanese POIs in OSM data is weak, leading to the least favorable performance in Tokyo.

From the visualization results of OSM data retrieval lo-

calization in Figure 5, it is evident that our method can locate specific store information or similar road details based on effective textual descriptions. Additionally, the heatmap responses provided by the Explainable Retrieval Module (ERM) show which features the model focuses on in the retrieved image. In the first example, the model focuses on "Burger Mania". Interestingly, even in non-top-1 results, it still emphasizes the burger icon. In the second example, the model focuses on the "zebra crossing" and "white gridline", with the first three retrieval results all highlighting the zebra crossing, and the best retrieval result matching both features. The ERM module also leverages the capabilities of LLMs to provide corresponding retrieval reasoning, such as matching the same store information or scene features, which significantly enhances the interpretability of the retrieval localization. Additional visual results comparing different methods are available in the supplementary material.

## 5.3. Ablation Studies

We evaluated the text synthetic effects of those directly generated by GPT versus those generated through the integrated process of CVG-Text, as shown in Table 3. CVG-Text exhibits higher text length and vocabulary complexity (TTR), with lower text similarity, indicating better text quality. The inclusion of OCR assistance helps precisely capture textual details in street view images, reducing GPT's tendency for vague descriptions and hallucinations, and effectively gen-





## References

- [1] Sameer Agarwal, Yasutaka Furukawa, Noah Snavely, Ian Simon, Brian Curless, Steven M Seitz, and Richard Szeliski. Building rome in a day. *Communications of the ACM*, 54(10):105–112, 2011. 1
- [2] Peter Anderson, Qi Wu, Damien Teney, Jake Bruce, Mark Johnson, Niko Sünderhauf, Ian Reid, Stephen Gould, and Anton Van Den Hengel. Vision-and-language navigation: Interpreting visually-grounded navigation instructions in real environments. In *Proceedings of the IEEE conference on computer vision and pattern recognition*, pages 3674–3683, 2018. 2
- [3] Anthropic. The claude 3 model family: Opus, sonnet, haiku, 2024. Accessed: 2024-09-23. 3
- [4] Anh-Quan Cao, Maximilian Jaritz, Matthieu Guillaumin, Raoul de Charette, and Loris Bazzani. Latteclip: Unsupervised clip fine-tuning via lmm-synthetic texts. *arXiv preprint arXiv:2410.08211*, 2024. 2, 3
- [5] Hila Chefer, Shir Gur, and Lior Wolf. Generic attention-model explainability for interpreting bi-modal and encoder-decoder transformers. In *Proceedings of the IEEE/CVF International Conference on Computer Vision*, pages 397–406, 2021. 6
- [6] Howard Chen, Alane Suhr, Dipendra Misra, Noah Snavely, and Yoav Artzi. Touchdown: Natural language navigation and spatial reasoning in visual street environments. In *Proceedings of the IEEE/CVF Conference on Computer Vision and Pattern Recognition*, pages 12538–12547, 2019. 2
- [7] Jiaqi Chen, Daniel Barath, Iro Armeni, Marc Pollefeys, and Hermann Blum. ” where am i?” scene retrieval with language. *arXiv preprint arXiv:2404.14565*, 2024. 1
- [8] Lin Chen, Jinsong Li, Xiaoyi Dong, Pan Zhang, Conghui He, Jiaqi Wang, Feng Zhao, and Dahua Lin. Sharegpt4v: Improving large multi-modal models with better captions. *arXiv preprint arXiv:2311.12793*, 2023. 2
- [9] Meng Chu, Zhedong Zheng, Wei Ji, and Tat-Seng Chua. Towards natural language-guided drones: Geotext-1652 benchmark with spatially relation matching. *arXiv preprint arXiv:2311.12751*, 2023. 3, 4
- [10] Fabian Deuser, Konrad Habel, and Norbert Oswald. Sample4geo: Hard negative sampling for cross-view geo-localisation. In *Proceedings of the IEEE/CVF International Conference on Computer Vision (ICCV)*, pages 16847–16856, 2023. 1, 2, 6, 8
- [11] Zi-Yi Dou, Yichong Xu, Zhe Gan, Jianfeng Wang, Shuohang Wang, Lijuan Wang, Chenguang Zhu, Pengchuan Zhang, Lu Yuan, Nanyun Peng, et al. An empirical study of training end-to-end vision-and-language transformers. In *Proceedings of the IEEE/CVF Conference on Computer Vision and Pattern Recognition*, pages 18166–18176, 2022. 3
- [12] Yuxin Fang, Quan Sun, Xinggang Wang, Tiejun Huang, Xinlong Wang, and Yue Cao. Eva-02: A visual representation for neon genesis. *Image and Vision Computing*, 149:105171, 2024. 6
- [13] Jan-Michael Frahm, Pierre Fite-Georgel, David Gallup, Tim Johnson, Rahul Raguram, Changchang Wu, Yi-Hung Jen, Enrique Dunn, Brian Clipp, Svetlana Lazebnik, et al. Building rome on a cloudless day. In *Computer Vision—ECCV 2010: 11th European Conference on Computer Vision, Heraklion, Crete, Greece, September 5–11, 2010, Proceedings, Part IV 11*, pages 368–381. Springer, 2010. 1
- [14] Owen He, Ansh Jain, Axel Adonai Rodriguez-Leon, Arnav Taduvayi, and Matthew Louis Mauriello. From crowdsourcing to large multimodal models: Toward enhancing image data annotation with gpt-4v. 2023. 2, 3
- [15] Lei Huang, Weijiang Yu, Weitao Ma, Weihong Zhong, Zhangyin Feng, Haotian Wang, Qianglong Chen, Weihua Peng, Xiaocheng Feng, Bing Qin, et al. A survey on hallucination in large language models: Principles, taxonomy, challenges, and open questions. *arXiv preprint arXiv:2311.05232*, 2023. 2, 3
- [16] Arnold Irschara, Christopher Zach, Jan-Michael Frahm, and Horst Bischof. From structure-from-motion point clouds to fast location recognition. In *2009 IEEE Conference on Computer Vision and Pattern Recognition*, pages 2599–2606. IEEE, 2009. 1
- [17] Wonjae Kim, Bokyung Son, and Ildoo Kim. Vilt: Vision-and-language transformer without convolution or region supervision. In *International conference on machine learning*, pages 5583–5594. PMLR, 2021. 6
- [18] Diederik P Kingma. Adam: A method for stochastic optimization. *arXiv preprint arXiv:1412.6980*, 2014. 6
- [19] Manuel Kolmet, Qunjie Zhou, Aljoša Ošep, and Laura Leal-Taixé. Text2pos: Text-to-point-cloud cross-modal localization. In *Proceedings of the IEEE/CVF Conference on Computer Vision and Pattern Recognition*, pages 6687–6696, 2022. 1, 2, 6
- [20] Junnan Li, Dongxu Li, Caiming Xiong, and Steven Hoi. Blip: Bootstrapping language-image pre-training for unified vision-language understanding and generation. In *International conference on machine learning*, pages 12888–12900. PMLR, 2022. 6
- [21] Kunpeng Li, Yulun Zhang, Kai Li, Yuanyuan Li, and Yun Fu. Visual semantic reasoning for image-text matching. In *Proceedings of the IEEE/CVF international conference on computer vision*, pages 4654–4662, 2019. 3
- [22] Weijia Li, Yawen Lai, Linning Xu, Yuanbo Xiangli, Jinhua Yu, Conghui He, Gui-Song Xia, and Dahua Lin. Omniscity: Omnipotent city understanding with multi-level and multi-view images. In *Proceedings of the IEEE/CVF Conference on Computer Vision and Pattern Recognition*, pages 17397–17407, 2023. 2
- [23] Weijia Li, Jun He, Junyan Ye, Huaping Zhong, Zhi-meng Zheng, Zilong Huang, Dahua Lin, and Conghui He. Crossviewdiff: A cross-view diffusion model for satellite-to-street view synthesis. *arXiv preprint arXiv:2408.14765*, 2024. 2
- [24] Liu Liu and Hongdong Li. Lending orientation to neural networks for cross-view geo-localization. In *Proceedings of the IEEE/CVF conference on computer vision and pattern recognition*, pages 5624–5633, 2019. 4
- [25] Simon Lynen, Bernhard Zeisl, Dror Aiger, Michael Bosse, Joel Hesch, Marc Pollefeys, Roland Siegwart, and Torsten

- Sattler. Large-scale, real-time visual-inertial localization revisited. *The International Journal of Robotics Research*, 39(9):1061–1084, 2020. 1
- [26] Shunji Mori, Ching Y Suen, and Kazuhiko Yamamoto. Historical review of ocr research and development. *Proceedings of the IEEE*, 80(7):1029–1058, 1992. 2, 3
- [27] Pierre Moulon, Pascal Monasse, Romuald Perrot, and Renaud Marlet. Openmvg: Open multiple view geometry. In *Reproducible Research in Pattern Recognition: First International Workshop, RRRP 2016, Cancún, Mexico, December 4, 2016, Revised Selected Papers 1*, pages 60–74. Springer, 2017. 1
- [28] OpenAI. Hello gpt-4o. <https://openai.com/index/hello-gpt-4o/>, 2024. 2, 3
- [29] Lu Qi, Jason Kuen, Yi Wang, Jiuxiang Gu, Hengshuang Zhao, Philip Torr, Zhe Lin, and Jiaya Jia. Open world entity segmentation. *IEEE Transactions on Pattern Analysis and Machine Intelligence*, 45(7):8743–8756, 2022. 2, 3
- [30] Alec Radford, Jong Wook Kim, Chris Hallacy, Aditya Ramesh, Gabriel Goh, Sandhini Agarwal, Girish Sastry, Amanda Askell, Pamela Mishkin, Jack Clark, et al. Learning transferable visual models from natural language supervision. In *International conference on machine learning*, pages 8748–8763. PMLR, 2021. 3, 6, 8
- [31] Vipula Rawte, Amit Sheth, and Amitava Das. A survey of hallucination in large foundation models. *arXiv preprint arXiv:2309.05922*, 2023. 2, 3
- [32] Paul-Edouard Sarlin, Cesar Cadena, Roland Siegwart, and Marcin Dymczyk. From coarse to fine: Robust hierarchical localization at large scale. In *Proceedings of the IEEE/CVF conference on computer vision and pattern recognition*, pages 12716–12725, 2019. 1
- [33] Yujiao Shi, Liu Liu, Xin Yu, and Hongdong Li. Spatial-aware feature aggregation for image based cross-view geo-localization. *Advances in Neural Information Processing Systems*, 32, 2019. 6
- [34] Yujiao Shi, Xin Yu, Dylan Campbell, and Hongdong Li. Where am i looking at? joint location and orientation estimation by cross-view matching. In *Proceedings of the IEEE/CVF Conference on Computer Vision and Pattern Recognition*, pages 4064–4072, 2020. 2
- [35] Gemini Team, Rohan Anil, Sebastian Borgeaud, Yonghui Wu, Jean-Baptiste Alayrac, Jiahui Yu, Radu Soricut, Johan Schalkwyk, Andrew M Dai, Anja Hauth, et al. Gemini: a family of highly capable multimodal models. *arXiv preprint arXiv:2312.11805*, 2023. 3
- [36] Huilin Tian, Jingke Meng, Wei-Shi Zheng, Yuan-Ming Li, Junkai Yan, and Yunong Zhang. Loc4plan: Locating before planning for outdoor vision and language navigation. *arXiv preprint arXiv:2408.05090*, 2024. 1, 2
- [37] Xiaolong Wang, Runsen Xu, Zhuofan Cui, Zeyu Wan, and Yu Zhang. Fine-grained cross-view geo-localization using a correlation-aware homography estimator. *Advances in Neural Information Processing Systems*, 36, 2024. 1
- [38] Scott Workman, Richard Souvenir, and Nathan Jacobs. Wide-area image geolocation with aerial reference imagery. In *Proceedings of the IEEE International Conference on Computer Vision*, pages 3961–3969, 2015. 3, 4
- [39] Yan Xia, Yusheng Xu, Cheng Wang, and Uwe Stilla. Vpcnet: Completion of 3d vehicles from mls point clouds. *ISPRS Journal of Photogrammetry and Remote Sensing*, 174:166–181, 2021. 1
- [40] Yan Xia, Letian Shi, Zifeng Ding, Joao F Henriques, and Daniel Cremers. Text2loc: 3d point cloud localization from natural language. In *Proceedings of the IEEE/CVF Conference on Computer Vision and Pattern Recognition*, pages 14958–14967, 2024. 1, 2, 6
- [41] Zimin Xia, Yujiao Shi, Hongdong Li, and Julian FP Kooij. Adapting fine-grained cross-view localization to areas without fine ground truth. In *European Conference on Computer Vision*, pages 397–415. Springer, 2025. 2
- [42] Shuyu Yang, Yinan Zhou, Zhedong Zheng, Yaxiong Wang, Li Zhu, and Yujiao Wu. Towards unified text-based person retrieval: A large-scale multi-attribute and language search benchmark. In *Proceedings of the 31st ACM International Conference on Multimedia*, pages 4492–4501, 2023. 3
- [43] Junyan Ye, Jun He, Weijia Li, Zhutao Lv, Jinhua Yu, Haote Yang, and Conghui He. Skydiffusion: Street-to-satellite image synthesis with diffusion models and bev paradigm. *arXiv preprint arXiv:2408.01812*, 2024. 1
- [44] Junyan Ye, Qiyao Luo, Jinhua Yu, Huaping Zhong, Zhimeng Zheng, Conghui He, and Weijia Li. Sg-bev: Satellite-guided bev fusion for cross-view semantic segmentation. In *Proceedings of the IEEE/CVF Conference on Computer Vision and Pattern Recognition*, pages 27748–27757, 2024. 1
- [45] Junyan Ye, Zhutao Lv, Weijia Li, Jinhua Yu, Haote Yang, Huaping Zhong, and Conghui He. Cross-view image geolocation with panorama-bev co-retrieval network. *arXiv preprint arXiv:2408.05475*, 2024. 1, 2, 4
- [46] Junyan Ye, Baichuan Zhou, Zilong Huang, Junan Zhang, Tianyi Bai, Hengrui Kang, Jun He, Honglin Lin, Zihao Wang, Tong Wu, et al. Loki: A comprehensive synthetic data detection benchmark using large multimodal models. *arXiv preprint arXiv:2410.09732*, 2024. 3
- [47] Xiaohua Zhai, Basil Mustafa, Alexander Kolesnikov, and Lucas Beyer. Sigmoid loss for language image pre-training. In *Proceedings of the IEEE/CVF International Conference on Computer Vision*, pages 11975–11986, 2023. 6, 8
- [48] Beichen Zhang, Pan Zhang, Xiaoyi Dong, Yuhang Zang, and Jiaqi Wang. Long-clip: Unlocking the long-text capability of clip. In *European Conference on Computer Vision*, pages 310–325. Springer, 2025. 3, 5
- [49] Junwei Zheng, Ruiping Liu, Yufan Chen, Kunyu Peng, Chengzhi Wu, Kailun Yang, Jiaming Zhang, and Rainer Stiefelhagen. Open panoramic segmentation. In *European Conference on Computer Vision*, pages 164–182. Springer, 2025. 2
- [50] Zhedong Zheng, Yunchao Wei, and Yi Yang. University-1652: A multi-view multi-source benchmark for drone-based geo-localization. In *Proceedings of the 28th ACM international conference on Multimedia*, pages 1395–1403, 2020. 4
- [51] Zhedong Zheng, Liang Zheng, Michael Garrett, Yi Yang, Mingliang Xu, and Yi-Dong Shen. Dual-path convolutional image-text embeddings with instance loss. *ACM Transac-*

*tions on Multimedia Computing, Communications, and Applications (TOMM)*, 16(2):1–23, 2020. [3](#)

- [52] Baichuan Zhou, Haote Yang, Dairong Chen, Junyan Ye, Tianyi Bai, Jinhua Yu, Songyang Zhang, Dahua Lin, Conghui He, and Weijia Li. Urbench: A comprehensive benchmark for evaluating large multimodal models in multi-view urban scenarios. *arXiv preprint arXiv:2408.17267*, 2024. [3](#)
- [53] Sijie Zhu, Taojiannan Yang, and Chen Chen. Vigor: Cross-view image geo-localization beyond one-to-one retrieval. In *Proceedings of the IEEE/CVF Conference on Computer Vision and Pattern Recognition*, pages 3640–3649, 2021. [2](#), [3](#), [4](#)